

## *Electronic Supplementary Information*

### **Flower-like Cobalt Carbide for Efficient Photothermal Carbon Dioxide Conversion**

Qing Guo,<sup>‡,a,c</sup> Shu-Guang Xia,<sup>‡,a,c</sup> Xu-Bing Li,<sup>\*,a,c</sup> Yang Wang,<sup>a,c</sup> Fei Liang,<sup>b,c</sup> Zhe-Shuai Lin,<sup>b,c</sup> Chen-Ho Tung<sup>a,c</sup> and Li-Zhu Wu<sup>\*,a,c</sup>

<sup>a</sup>Key Laboratory of Photochemical Conversion and Optoelectronic Materials, Technical Institute of Physics and Chemistry, the Chinese Academy of Sciences, Beijing 100190, P. R. China

<sup>b</sup>Key Laboratory of Functional Crystals and Laser Technology, Technical Institute of Physics and Chemistry, Chinese Academy of Sciences, Beijing 100190, P. R. China

<sup>c</sup>School of Future Technology, University of Chinese Academy of Sciences, Beijing 100049, P. R. China

*\*To whom correspondence should be addressed.*

*E-mail: lixubing@mail.ipc.ac.cn; lzwu@mail.ipc.ac.cn;*

*Telephone: (+86) 10-8254-3579; Fax: (+86) 10-8254-3580.*

## Table of Contents

1. Materials
2. Instruments
3. Preparation of Co<sub>2</sub>C nanoflowers
4. Experimental detail of XSA spectroscopy
5. DFT calculations
6. Photothermal catalytic cycloaddition reaction
7. Atomic force microscopy measurement
8. Elemental mapping of Co<sub>2</sub>C
9. FT-IR image of Co<sub>2</sub>C samples before and after calcination
10. XPS spectroscopy of prepared Co<sub>2</sub>C nanoflowers
11. High-resolution XPS spectra of Co 2p for Co<sub>2</sub>C
12. High-resolution XPS spectra of O 1s for Co<sub>2</sub>C
13. Fitting parameters of Co *K*-edge EXAFS
14. DRS measurement of the Co<sub>2</sub>C
15. Photothermal heating curves of water
16. Temperature of acetonitrile solution
17. Comparison of cycloaddition reaction activity for Co<sub>2</sub>C under light irradiation and heating
18. Stability tests of reaction system
19. Adsorption behavior of substrates on Co<sub>2</sub>C
20. Calculation of photothermal conversion efficiency
21. Summary of photothermal conversion efficiency of various materials
22. Epoxides with different substituents
23. CO<sub>2</sub> cycloaddition with epoxide catalyzed by various materials
24. Reference

## 1. Materials

Anhydrous cobalt acetate ( $\text{CoAc}_2$ , 98%), oleylamine (OAm approximate, C18-content 80-90%) and triethylene glycol (3-EG, 99%) were purchased from Alfa and used as received. Epichlorohydrin (99%) was purchased from Innochem and tetrabutylammonium bromide (TBAB, 99%) was obtained from Across and used as received. Other chemicals are of analytical grade without any further purification unless otherwise noted.

## 2. Instruments

High-resolution transmission electron microscopy (HRTEM) was performed by JEM 2100F (operated at an accelerating voltage of 200 kV). Scanning electron microscopy (SEM) was performed by TESCAN MIRA3. The X-ray photoelectron spectra (XPS) measurements were performed on an ESCALAB 250 spectrophotometer with  $\text{Al-K}\alpha$  radiation. The binding energy scale was using the C 1s peak at 284.6 eV. X-ray powder diffraction pattern (XRD) was carried out on a Bruker AXS D8 X-ray diffractometer (parameters:  $\text{Cu K}\alpha$ ,  $\lambda = 1.5406 \text{ \AA}$ , 100 mA, and 40 kV). UV-vis diffuse reflectance spectra (DRS) was carried out by Cary 5000 UV-visible NIR spectrophotometer employing a lab-sphere diffuse reflectance accessory over the range 300-1200 nm. Photothermal study was performed by using a 635 nm continuous-wave semiconductor laser as light source (BWT Beijing, China). The temperature of the solution was detected using a thermocouple probe with an accuracy of 0.1 °C and recorded by a digital thermometer every second. The thermal imaging of the sample was performed using an infrared camera (Ti400). The power density of laser irradiation was measured by a digital power meter (PM100D, Thorlabs, USA). Fourier transform infrared spectroscopy (FT-IR) spectra were performed on FT-IR spectrometer (Excalibur 3100) with a KBr disk containing  $\text{Co}_2\text{C}$  powder. X-ray absorption spectroscopic (XAS) data was collected at Beam line 1W2B of the Beijing Synchrotron Radiation Facility (BSRF).

## 3. Preparation of $\text{Co}_2\text{C}$ nanoflowers

$\text{Co}_2\text{C}$  nanoflowers were prepared referring to previous method.<sup>1</sup> In a typical reaction, Anhydrous cobalt acetate ( $\text{CoAc}_2$ ) was added into a 50 mL round-bottom flask, which was chosen as cobalt precursor. Then, the mixture of triethylene glycol (3-EG) and oleylamine (OAm) were added to the flask, which was heated to 300 °C using heating mantle under argon atmosphere for about 3.0 h. Subsequently, it was cooled to room temperature. After that the reaction solution was centrifuged (5000

rpm, 5.0 minutes) to separate the lamellar Co<sub>2</sub>C samples from the supernatant. The obtained samples were washed with a mixture of n-hexane and acetone for several times. Finally, the Co<sub>2</sub>C samples were calcinated at 340 °C for 5.0 h with a heating rate of 2.0 °C min<sup>-1</sup> under a flow of 30 mL/min N<sub>2</sub> atmosphere to remove the surface organic ligands. After that, the samples were collected for further characterizations and applications.

#### 4. The experimental detail of XSA spectroscopy

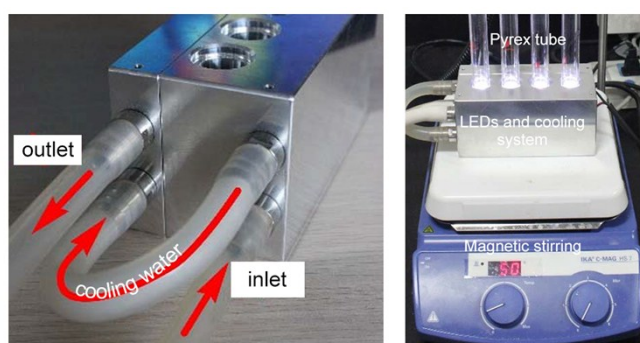
XAS spectroscopy was acquired at beamline 1W1B, Beijing Synchrotron Radiation Facility (BSRF). The X-ray source was 2.5 GeV with a current of 250 mA in top-up mode. Before XAS measurement, powder samples were evenly milled and smeared onto a metal-free polyimide tape. *K*-edge energy calibration was performed with a metallic cobalt foil standard. Using Si(111) double-crystal monochromator, the data collection was carried out in transmission mode using ionization chamber. Extended X-ray absorption fine structure (EXAFS) spectra were transformed into *R*-space by Athena software. Firstly, the XAS spectra were obtained by subtracting the pre-edge background (-150 to -50 eV vs. absorption edge) from the overall absorption and then normalized with range of 150-700 eV. Subsequently,  $\chi(k)$  data in the *k*-space were Fourier transformed to *R*-space using a hanning window (*k*-weight = 2, *k* is ranged from 3.0 to 12.0 Å<sup>-1</sup>) to separate the EXAFS contributions from different coordination shells.

#### 5. DFT calculations

The first-principles calculations of the work were conducted by using the pseudopotential methods<sup>2</sup> implemented in the CASTEP package<sup>3</sup>, basing on the density functional theory (DFT).<sup>4</sup> Through the BFGS method, the atomic positions and cell parameters in the unit cells of all crystals were fully optimized.<sup>5</sup> In order to simulate ion-electron interactions, the optimized ultrasoft pseudopotentials<sup>6</sup> were used for all constituent elements. A kinetic energy cutoff was chosen as 400 eV with Monkhorst-Pack *k*-point meshes spanning less than 0.04/Å<sup>3</sup> in the Brillouin zone.<sup>7</sup> The convergence thresholds between optimization cycles for energy change, maximum force, maximum stress, and maximum displacement were set as 5.0 × 10<sup>-6</sup> eV/atom, 0.01 eV/Å, 0.02 GPa, and 5.0 × 10<sup>-4</sup> Å, respectively. When all of these criteria were satisfied, the optimization terminated. The imaginary part of the dielectric function was calculated and the real part of the dielectric function was determined by the Kramers–Kronig transform based on the optimized geometry structure.<sup>8</sup>

## 6. Photothermal catalytic cycloaddition reaction

Briefly, 25.0 mg  $\text{Co}_2\text{C}$  powders were dispersed into 3.0 mL acetonitrile in a 20 mL Pyrex tube. Then, 0.25 mmol tetra-*n*-butylammonium bromide (TBAB) was introduced into the solution. The Pyrex tube was sealed and bubbled with  $\text{CO}_2$  gas for 20 min. Subsequently, 0.15 mmol epichlorohydrin was injected into solution by using a microinjector. Finally, the Pyrex tube was irradiated by blue LEDs ( $\lambda = 450 \text{ nm}$ ;  $100 \text{ mW cm}^{-2}$ ) for 15 h. The setup of the photoreactor was below. After reaction, the solution was filtered to remove catalyst by filter membrane, which was then evaporated under reduced pressure to give the desired product.



Note: The photoreactor used in our system. (Left: illustration of the water-cooling system. Right: Pyrex tube, light source, and magnetic stirring.

## 7. AFM measurement

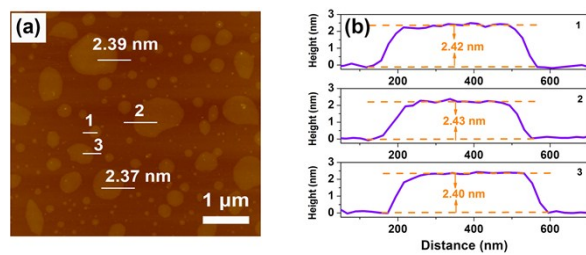


**Figure S1.** AFM image of obtained  $\text{Co}_2\text{C}$  (a) and the corresponding height profiles (b).

## 8. Elemental mapping of $\text{Co}_2\text{C}$

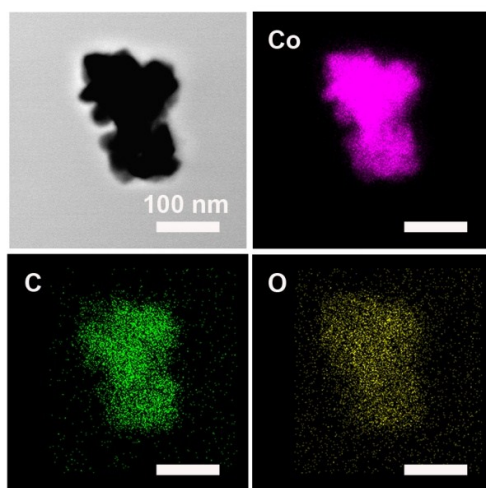


**Figure S2.** TEM image of  $\text{Co}_2\text{C}$  and corresponding elemental mapping of Co, C and O, respectively. As shown in Figure S1, the coexistence of Co, C and O was revealed, suggesting the formation of  $\text{Co}_2\text{C}$  with trace amount of  $\text{Co}(\text{OH})_2$ .

### 9. FT-IR image of Co<sub>2</sub>C samples before and after calcination

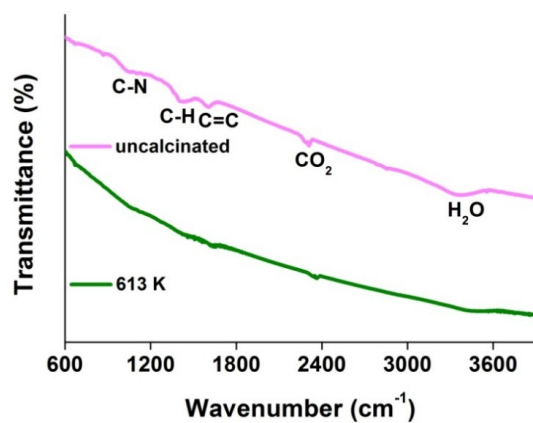


**Figure S3.** FT-IR image of Co<sub>2</sub>C samples before and after calcination at 613 K under N<sub>2</sub> atmosphere. As shown in Figure S2, the peaks at 1630, 1420 and 1050 cm<sup>-1</sup> attributed to the vibration of C=C, C-H and C-N respectively have disappeared after calcination, suggesting that the organic ligands on the surface of Co<sub>2</sub>C were removed.



## 10. XPS spectroscopy of prepared Co<sub>2</sub>C nanoflowers

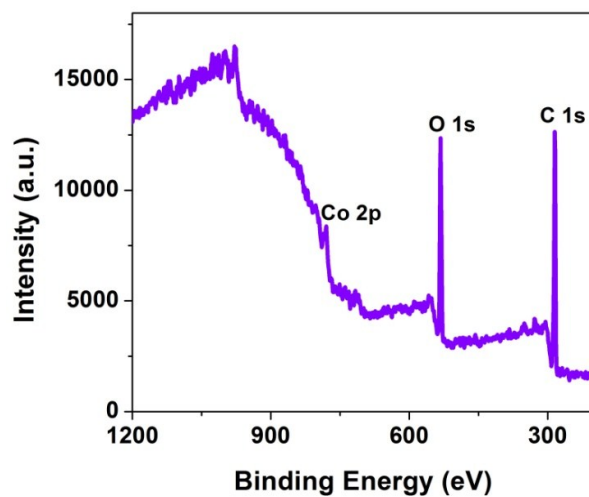


**Figure S4.** Full X-ray photoelectron spectroscopy of the prepared Co<sub>2</sub>C nanoflowers.

## 11. High-resolution XPS spectra of Co 2p for Co<sub>2</sub>C

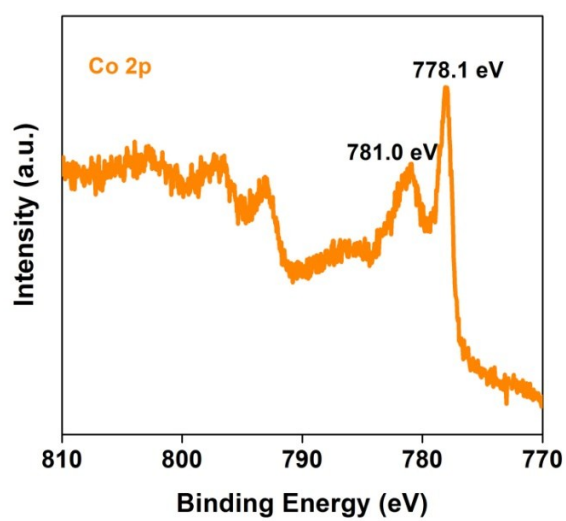


**Figure S5.** High-resolution XPS spectra of Co 2p for the obtained Co<sub>2</sub>C sample. As shown in Figure S4, the peak at 781.0 eV and 778.1 eV can be attributed to Co(OH)<sub>2</sub> and carbidic Co in Co<sub>2</sub>C.<sup>9</sup>

## 12. High-resolution XPS spectra of O 1s for Co<sub>2</sub>C

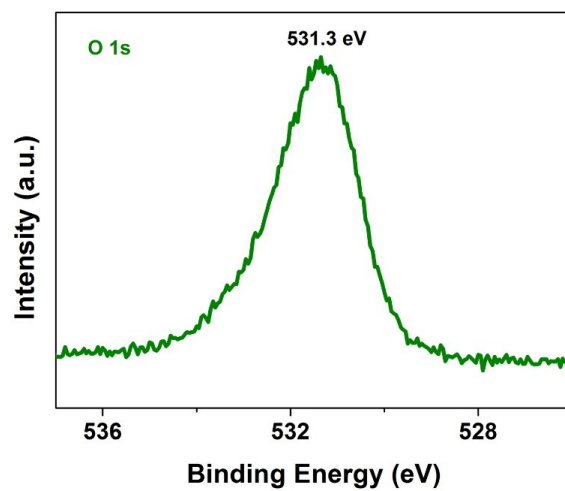


**Figure S6.** High-resolution XPS spectra of O 1s for the obtained Co<sub>2</sub>C sample. As shown in Figure S5, the peak at 531.3 eV can be assigned to hydroxide ions on the surface of Co<sub>2</sub>C.<sup>9,10</sup>

### 13. Fitting parameters of Co K-edge EXAFS

For the fitting processes, the data range of  $k$  and  $R$  is 3.0-12  $\text{\AA}^{-1}$  and 1.2-2.9  $\text{\AA}$ , respectively. The  $R$ -factor  $R_f$  for fitting is 0.00542, 0.00458 and 0.00642 for Co-C, Co-Co1 and Co-Co2, respectively.<sup>11</sup>

**Table S1.** Detailed fitting parameters of the Co K-edge EXAFS.

|       | Coordination Numbers (C.N.) | Radial Distance ( $\text{\AA}$ ) | $S_0^2$ | $\sigma^2$ |
|-------|-----------------------------|----------------------------------|---------|------------|
| Co-C  | 2.00                        | 1.89                             | 1.497   | 0.00259    |
| Co-O  | 6.20                        | 2.54                             | 4.638   | 0.01433    |
| Co-Co | 5.25                        | 2.71                             | 3.929   | 0.0134     |

#### 14. DRS measurement of the synthesized Co<sub>2</sub>C nanoflowers

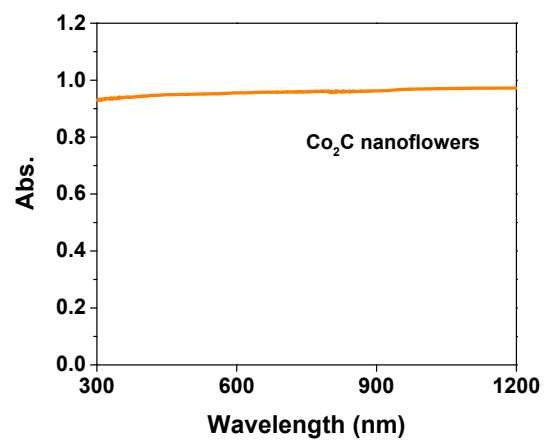


**Figure S7.** UV-vis-NIR diffuse reflectance spectroscopy (DRS) measurement of the synthesized Co<sub>2</sub>C nanoflowers.

## 15. Photothermal heating curves of water

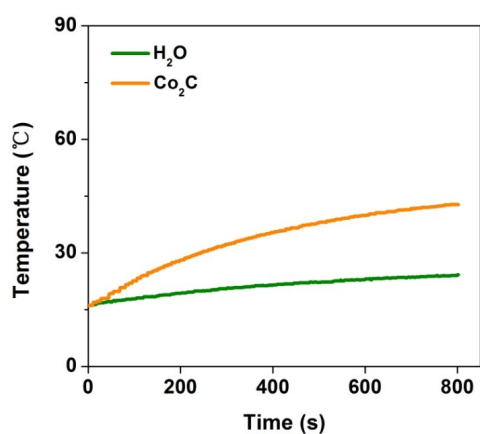


**Figure S8.** Photothermal heating curves of pure water and Co<sub>2</sub>C water suspension under the irradiation of 635 nm laser with a power density of 0.5 W cm<sup>-2</sup>. As shown in Figure S7, the temperature of pure H<sub>2</sub>O only slightly increased to 24 °C in 13 min irradiation.

## 16. Temperature of acetonitrile solution

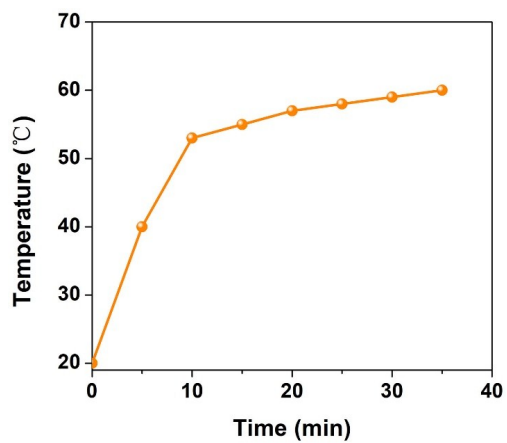


**Figure S9.** Temperatures of acetonitrile solution (3 mL) with Co<sub>2</sub>C (25 mg) under blue LEDs irradiation ( $\lambda = 450$  nm), which were measured by thermometer.

### 17. Comparison of cycloaddition reaction activity for CO<sub>2</sub>C under light irradiation and heating

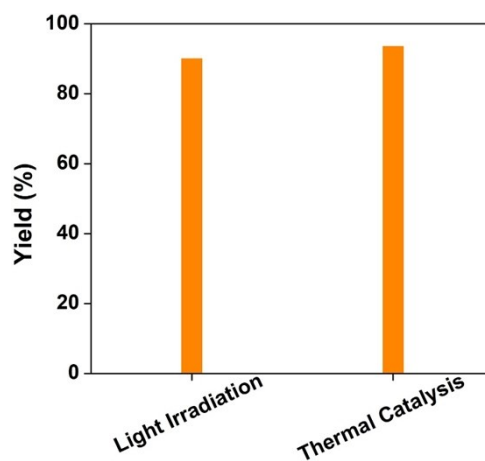


**Figure S10.** Comparison of products yield of CO<sub>2</sub> and 3-chloridepropylene oxide cycloaddition reaction for CO<sub>2</sub>C catalysis under photothermal heating (with visible light irradiation) and direct heating at 60 °C (without visible light irradiation). As shown in Figure S9, product yields were similar for light irradiation and thermal catalysis, giving the convincing evidence for the photothermal pathway of cycloaddition reaction, rather than photocatalysis.



## 18. Stability tests of reaction system

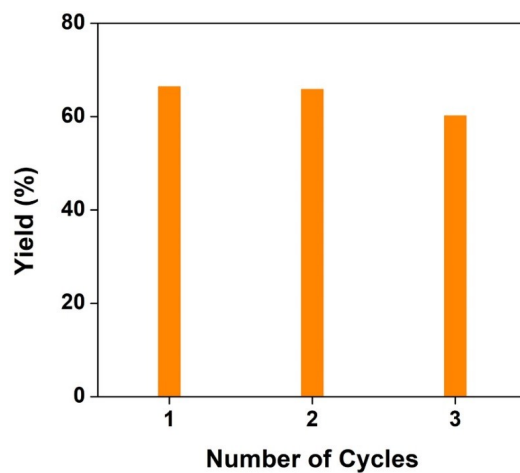


**Figure S11.** The stability test of  $\text{Co}_2\text{C}$  catalytic  $\text{CO}_2$  cycloaddition reaction under AM 1.5 irradiation, the addition of 0.5 mmol TBAB into system after each cycle. As shown in Figure S10, the slight decline of carbonate yield after 3 recycles indicated the stability of the reaction system. Reaction conditions:  $\text{Co}_2\text{C}$  50 mg, TBAB 0.5 mmol, epichlorohydrin 0.15 mmol, AM 1.5, 24 h.

### 19. Adsorption behaviour of substrates on $\text{Co}_2\text{C}$ (101)

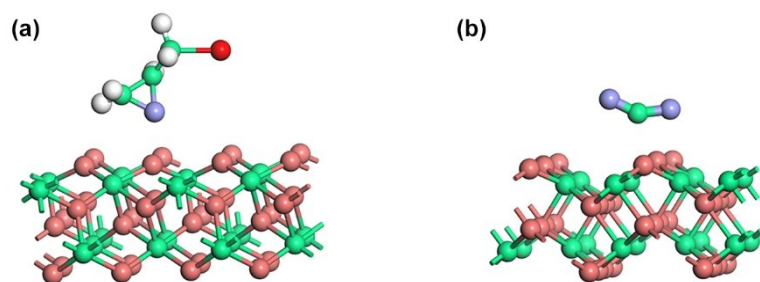


**Figure S12.** The interaction of (a) epichlorohydrin and (b)  $\text{CO}_2$  molecule with  $\text{Co}_2\text{C}$ , respectively. Brown, green, blue, white and red balls denote cobalt, carbon, oxygen, hydrogen and chlorine atom, respectively.

## 20. Calculation of photothermal conversion efficiency

According to precious reports,<sup>12-14</sup> the total energy change of the system can be defined as follows:

$$\sum_i m_i C_{p,i} dT/dt = Q_{Co2C} + Q_0 - Q_{amb} \quad (1)$$

where  $m$  and  $C_p$  are the mass and heat capacity of water,  $T$  is the solution temperature,  $Q_{Co2C}$  is the heat input of the absorbed laser energy by  $Co_2C$  nanoflowers,  $Q_0$  is the energy absorbed by the sample vial and solvent, and  $Q_{amb}$  is the sum of heat dissipated to the surrounding environment.

The energy input from  $Co_2C$  calculated using Equation S2,

$$Q_{Co2C} = I (1-10^{-A}) \eta \quad (2)$$

Where  $I$  refers to the incident power density of 635 nm laser irradiation,  $A$  is the absorbance of  $Co_2C$  at 635 nm, and  $\eta$  is the photothermal conversion efficiency of  $Co_2C$  at 635 nm.

$$Q_{amb} = hS (T - T_{amb}) \quad (3)$$

Where  $h$  is heat transfer coefficient,  $S$  is the surface area of the container, and  $T_{amb}$  is ambient temperature of the surrounding.

Since the heat output  $Q_{amb}$  is increased along with the increase of the temperature according to the Equation S3, the system temperature will rise to a maximum when the heat input is equal to heat output:

$$Q_{Co2C} + Q_0 = Q_{amb,max} = hS (T_{max} - T_{amb}) \quad (4)$$

Where  $T_{max}$  is the equilibrium temperature, photothermal conversion efficiency at 635 nm can be expressed to

$$\eta = hS (T_{max} - T_{amb}) - Q_0 / I (1-10^{-A}) \quad (5)$$

In order to get  $hS$ , a dimensional driving force temperature  $\Theta$  is defined

$$\Theta = (T_{amb} - T) / (T_{amb} - T_{max}) \quad (6)$$

And a sample system time constant  $\tau_s$  is defined as  $\tau_s = \sum_i m_i C_{p,i} / hS$ , which is substituted into Equation (1) and rearranged to yield following equation:

$$d\Theta/dt = [(Q_{Co2C} + Q_0) / hS(T_{max} - T_{amb}) - \Theta] / \tau_s \quad (7)$$

At the cooling period of  $Co_2C$  aqueous dispersion, the light source was shut off,  $Q_{Co2C} + Q_0 = 0$ ,

$$dt = -\tau_s d\Theta/\Theta, \text{ and } t = -\tau_s \ln\Theta \quad (8)$$

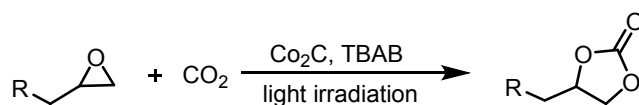
Time constant was determined to be  $\tau_s = 479$  s by applying the linear time data from the cooling stage (1000 s) versus negative natural logarithm of driving force temperature (Figure 2e). In addition, the  $m$  is 1.0 g and  $C_p$  is 4.2 J/g,  $hS$  is calculated to be 8.77 mW/°C. Thus, photothermal conversion efficiency ( $\eta$ ) of  $Co_2C$  can be dined as ~63.1% at 635 nm.

## 21. Summary of photothermal conversion efficiency of various materials

**Table S2.** Comparison of  $\eta$  value of the flower-like Co<sub>2</sub>C with reported materials.

| Samples                            | Photothermal efficiency ( $\eta$ , %) | Wavelength of laser (nm) | Reference   |
|------------------------------------|---------------------------------------|--------------------------|---|
| Ti <sub>3</sub> C <sub>2</sub>     | 30.6                                  | 808                      | <i>Nano Lett.</i> <b>2017</b> , <i>17</i> , 384-391.              |
| Nb <sub>2</sub> C                  | 36.4                                  | 808                      | <i>J. Am. Chem. Soc.</i> <b>2017</b> , <i>139</i> , 16235-16247.  |
|                                    | 45.65                                 | 1064                     |   |
| Ni <sub>3</sub> C                  | 16.9                                  | 808                      | <i>Nanoscale</i> <b>2014</b> , <i>6</i> , 12591-12600             |
| Au-Fe <sub>2</sub> C               | 30.2                                  | 808                      | <i>ACS Nano.</i> <b>2017</b> , <i>11</i> , 9239-9248              |
| Au nanorods                        | 21                                    | 808                      | <i>Angew. Chem. Int. Ed.</i> <b>2013</b> , <i>52</i> , 4169-4173. |
| Au nanoshells                      | 13                                    | 808                      | <i>Angew. Chem. Int. Ed.</i> <b>2013</b> , <i>52</i> , 4169-4173. |
| Cu <sub>2-x</sub> Se NCs           | 22                                    | 808                      | <i>Nano Lett.</i> <b>2011</b> , <i>11</i> , 2560-2566.            |
| Cu <sub>9</sub> S <sub>5</sub> NCs | 25.7                                  | 980                      | <i>ACS Nano</i> <b>2011</b> , <i>5</i> , 9761-9771.               |
| PEG-BDP/NPs                        | 48.3                                  | 650                      | <i>J. Mater. Chem. B</i> , <b>2019</b> , <i>7</i> , 4528-4537.    |
| <b>Co<sub>2</sub>C</b>             | <b>63.1</b>                           | <b>635</b>               | <b>This work</b>  |

**22. Table S3 Catalytic activity of Co<sub>2</sub>C for CO<sub>2</sub> and epoxides cycloaddition reaction with different substituents<sup>a</sup>**



| Entry | R  | Time (h) | Yield (%)         |
|-------|--|----------|-------------------|
| 1     | -Cl  | 15       | 93.5              |
| 2     | -Br  | 15       | 94.8              |
| 3     | -OH  | 48       | 69.2              |
| 4     | -Ph  | 48       | 62                |
| 5     | -(CH <sub>2</sub> ) <sub>2</sub> CH <sub>3</sub> | 26       | 77                |
| 6     | -OPh   | 36       | 69.4 <sup>b</sup> |

<sup>a</sup>Reaction conditions: 25 mg Co<sub>2</sub>C, 0.25 mmol TBAB, 0.15 mmol propylene oxide with different substituents, blue LEDs irradiation. <sup>b</sup>The reaction was carried out with 45 mg Co<sub>2</sub>C, 0.4 mmol TBAB and 0.15 mmol propylene oxide, blue LEDs irradiation. The yield of products was analyzed by <sup>1</sup>H NMR with diphenylmethanol, according to the equation of [ $\eta$  (%) = n(carbonate)/n(3-chloropropylene oxide) × 100%].

### 23. CO<sub>2</sub> cycloaddition with epoxide catalyzed by various materials

**Table S4.** Comparison of CO<sub>2</sub> cycloaddition reaction yield with other catalysts.

| Catalyst                                  | Condition        | Reaction yield (%) | Reference  |
|---|------------------|--------------------|--|
| Co@AP/HMTA-0.20                           | 100 °C           | 99.5               | <i>Adv. Mater.</i> <b>2017</b> , <i>29</i> , 1700445.            |
| Co-CMP                                    | 100 °C           | 98.1               | <i>Nat. Commun.</i> <b>2013</b> , <i>4</i> , 1960.               |
| ZIF-8                                     | 80 °C            | 73.1               | <i>ACS Catal.</i> <b>2012</b> , <i>2</i> , 180-183.              |
| ZIF-8/Carbon Nitride Foam                 | 80 °C            | 100                | <i>Adv. Funct. Mater.</i> <b>2017</b> , <i>27</i> , 1700706.     |
| MA500                                     | 150 °C           | 86.9               | <i>Appl. Catal. B: Environ</i> <b>2019</b> , <i>241</i> , 41–51. |
| Zn powder                                 | 80 °C            | 92                 | <i>Eur. J. Org. Chem.</i> <b>2019</b> , 1311–1316                |
| T5 (Charge-Containing Thiourea Catalysts) | 90 °C            | 98                 | <i>J. Org. Chem.</i> <b>2018</b> , <i>83</i> , 9991-10000.       |
| HPC-800                                   | Full-arc Xe lamp | 94                 | <i>Angew. Chem. Int. Ed.</i> <b>2019</b> , <i>58</i> , 3511-3515 |
| <b>Co<sub>2</sub>C</b>                    | <b>Blue LEDs</b> | <b>93.5</b>        | <b>This work</b>   |
|   | <b>60 °C</b>     | <b>94.8</b>        |  |

## 24. Reference

1. Z. J. Huba and E. E. Carpenter, *CrystEngComm* **2014**, *16*, 8000-8007.
2. M. C. Payne, M. P. Teter, D. C. Allan, T. A. Arias and J. D. Joannopoulos, *Rev. Mod. Phys.* **1992**, *64*, 1045-1097.
3. D. J. Heldebrant, P. K. Koech, V.-A. Glezakou, R. Rousseau, D. Malhotra and D. C. Cantu, *Chem. Rev.* **2017**, *117*, 9594-9624.
4. W. Kohn, *Rev. Mod. Phys.* **1999**, *71*, 1253-1266.
5. B. G. Pfrommer, M. Côté, S. G. Louie and M. L. Cohen, *J. Comput. Phys.* **1997**, *131*, 233-240.
6. A. M. Rappe, K. M. Rabe, E. Kaxiras and J. D. Joannopoulos, *Phys. Rev. B* **1990**, *41*, 1227-1230.
7. H. J. Monkhorst and J. D. Pack, *Phys. Rev. B* **1976**, *13*, 5188-5192.
8. L. Kang, D. M. Ramo, Z. Lin, P. D. Bristowe, J. Qin and C. Chen, *J. Mater. Chem. C* **2013**, *1*, 7363-7370.
9. S. Li, C. Yang, Z. Yin, H. Yang, Y. Chen, L. Lin, M. Li, W. Li, G. Hu, D. Ma, *Nano Res.* **2017**, *10*, 1322-1328.
10. D. Gazzoli, M. Occhiuzzi, A. Cimino, D. Cordischi, G. Minelli, F. Pinzari, *J. Chem. Soc., Faraday Trans.* **1996**, *92*, 4567-4574.
11. M. Mikkelsen, M. Jørgensen and F. C. Krebs, *Energy Environ. Sci.* **2010**, *3*, 43-81.
12. H. Lin, X. Wang, L. Yu, Y. Chen and J. Shi, *Nano Lett* **2017**, *17*, 384-391.
13. H. Lin, S. Gao, C. Dai, Y. Chen and J. Shi, *J. Am. Chem. Soc.* **2017**, *139*, 16235-16247.
14. L. Yuwen, J. Zhou, Y. Zhang, Q. Zhang, J. Shan, Z. Luo, L. Weng, Z. Teng and L. Wang, *Nanoscale* **2016**, *8*, 2720-2726.